NREL National Renewable Energy Laboratory

Innovation for Our Energy Future

Si Passivation and Chemical Vapor Deposition of Silicon Nitride

Final Technical Report
March 18, 2007

H.A. Atwater
California Institute of Technology
Pasadena, California

Si Passivation and Chemical Vapor Deposition of Silicon Nitride

Final Technical Report
March 18, 2007

H.A. Atwater
California Institute of Technology
Pasadena, California

NREL Technical Monitor: R. Matson/F. Posey-Eddy
Prepared under Subcontract No. AAT-2-31605-01

Available electronically at http://www.osti.gov/bridge

Available for a processing fee to U.S. Department of Energy
and its contractors, in paper, from:
      U.S. Department of Energy
      Office of Scientific and Technical Information
      P.O. Box 62
      Oak Ridge, TN 37831-0062
      phone: 865.576.8401
      fax: 865.576.5728
      email: mailto:reports@adonis.osti.gov

Available for sale to the public, in paper, from:
      U.S. Department of Commerce
      National Technical Information Service
      5285 Port Royal Road
      Springfield, VA 22161
      phone: 800.553.6847
      fax: 703.605.6900
      email: orders@ntis.fedworld.gov
      online ordering: http://www.ntis.gov/ordering.htm

Table of Contents

List of Figures

List of Tables

Subcontract Executive Overview

This research program investigated chemical and physical methods for Si surface passivation for application in crystalline Si and thin Si film photovoltaic devices. Overall, our efforts during the project were focused in three areas: i) synthesis of silicon nitride thin films with high hydrogen content by hot wire chemical vapor deposition ii) investigation of the role of hydrogen passivation of defects in crystalline Si and Si solar cells by out diffusion from hydrogenated silicon nitride films iii) investigation of the growth kinetics and passivation of hydrogenated polycrystalline Si grown by hot wire chemical vapor deposition.

Work on hydrogen-passivated silicon nitride synthesis was applied to solar cell passivation in collaboration with industrial partners at Evergreen Solar and thin film silicon passivation in collaboration with BP Solar. By way of enumeration, under this contract 3 PhD theses were published, along with 16 journal publications. Researchers working under this subcontract have also been actively serving the photovoltaics technical community -- the Principal Investigator served as a co-organizer for the Materials Research Society Symposium A in 2006 and served as a subpanel chair for the DOE Basic Energy Sciences Workshop on Basic Research in Solar Energy Utilization in 2005.

1. Silicon Nitride Synthesis by Hot Wire Chemical Vapor Deposition:

Introduction

A major focus of our subcontract was on silicon nitride (SiN_x) films, which have been widely used in the semiconductor industry for use as a lithographic mask and gate dielectric. Particularly for gate dielectric applications, silicon nitride offers the advantage of lower deposition temperature (300^oC) as compared with other materials, avoiding the problems of impurity diffusion that can occur at conventional processing temperatures of 900^oC[1]. For photovoltaic applications, silicon nitride acts as an effective anti-reflection (AR) coating due to its high refractive index (2.0-2.5). These films may also serve as passivation coatings for surface and bulk defects in the underlying silicon, due to the large fraction of hydrogen that may be incorporated (up to 25 atomic %)[2].

A promising technique for low temperature SiN_x growth is hot-wire CVD (HWCVD), also known as catalytic CVD (Cat-CVD)[3]. Recent work on SiN_x growth by HWCVD has focused gate dielectric applications[1], with one group fabricating a thin-film transistor made entirely by this technique[4]. Our subcontract research focused on use of HWCVD SiN_x for photovoltaic applications, with particular attention paid to the refractive index and hydrogen content of the films.

Summary of Technical Accomplishments:

Silicon nitride films were grown by hot-wire chemical vapor deposition and film properties have been characterized as a function of SiH_4/NH_3 flow ratio. It was demonstrated that hot wire chemical vapor deposition leads to growth of SiN_x films with controllable stoichiometry and hydrogen. The following findings resulted from our subcontract research:

- The decomposition rate of NH_3 on tungsten is low relative to SiH_4, explaining the large excess flow of NH_3 needed to produce stoichiometric silicon nitride films.

- The NH_3 decomposition reaction is catalyzed, however, with an activation energy of 31 kcal/mole.

- Varying the ratio of SiH_4/NH_3 from 1-8% produced films ranging in refractive index from 1.8-2.5, with hydrogen content ranging from 9-18 atomic %.

- Transmission measurements using FTIR revealed an abrupt transition in the bonding of H (going from N to Si) in SiN_x as the flow ratio was increased beyond 6% SiH_4/NH_3. As this ratio was increased, the overall H-content increased in the film, suggesting that SiH_4 is the primary source of H under these conditions.

- Films deposited with a low flow ratio of SiH_4/NH_3 of 1% showed a prominent Si-O-Si feature suggesting post-growth oxidation, a result further confirmed with RBS, indicating 23% oxygen incorporation in the film.

- Post-deposition H_2 treatments were found to have little impact on the overall atomic percentage of H in the film, but did appear to have an etching effect with the Si-rich samples used.

- Annealing studies revealed different kinetics for H release from Si versus N, consistent with a mechanism involving bond dissociation, followed by molecular diffusion[9].

Experimental Approach

The system used in the deposition of SiN_x is a high vacuum chamber with a base pressure of order 10^{-9} Torr. Source gases, consisting of SiH_4 (diluted to 1% in He), NH_3 (and H_2 for post-deposition treatments) are introduced through a gas inlet and decomposed on a W wire (0.5 mm diameter, 12 cm length, 1800^oC temperature). Flow rates of the various gases range from 4-48 sccm, with SiH_4/NH_3 ratios ranging from 1-8%, and pressures in the range of 20-100 mTorr. A substrate heater is located approximately 5 cm from the wire, and a shutter is used to protect substrates from the evaporation of impurities from the wire during its initial heating; growth temperatures were approximately 300^oC for this study. The substrates used were lightly doped p-type (350 Ω-cm), double-side polished, float-zone Si. A quadrupole mass spectrometer is put in place of the substrate heater during experiments aimed at measuring radicals desorbed from the filament.

Radical Measurements – NH_3 Decomposition

As a means to probe the kinetics of NH_3 decomposition on the wire, low-pressure radical species measurements were made using a quadrupole mass spectrometer with the capability of tunable electron energy for selective radical ionization. This method is

detailed in another study by these authors[5]. Mass spectra were acquired of the NH_x species desorbed from the wire under conditions of 3×10^{-6} Torr NH_3, at a wire temperature of $2100^{\circ}C$. Even at such a high temperature, there is an extremely small yield of NH_2 produced from NH_3 decomposition. Relative to the decomposition probability of SiH_4 at a similar temperature, NH_3 is (at minimum) a factor of 10 less. This suggests that to produce stoichiometric (Si_3N_4) films, the feed gas must contain SiH_4 in a large dilution of NH_3, a common observation in the growth of these films[1,4]. The intensity of the NH_2 yield was also measured as a function of wire temperature, from $1550-2100^{\circ}C$. These data yield an approximate activation energy for the NH_3 decomposition reaction:

$$NH_3 + W = NH_2 + W\text{-}H \qquad\qquad (1)$$

where "W" represents a bare surface site on the W wire, and "W-H" is a hydrogenated surface site on the wire. The value of 31 kcal/mole obtained is significantly smaller than the known N-H bond dissociation energy of 93 kcal/mole[6], indicating that as with the reaction of SiH_4 to SiH_3[5], the reaction in Eqn. 1 is catalyzed.

Film Growth Results

SiN$_x$ films were initially prepared under conditions of 1.8% SiH_4 in NH_3 (16 sccm 1% SiH_4 mixture, 8.7 sccm NH_3), 20 mTorr total pressure, and a substrate temperature of $280^{\circ}C$, with a growth time of 60 minutes. Resulting films were analyzed with a single wavelength (633 nm) ellipsometer, yielding a thickness of 185 nm and refractive index of 1.8. Subsequent analysis was performed using X-ray Photoelectron Spectroscopy (XPS) to gain insight into the bonding structure of the film. A HWCVD and standard (stoichiometric nitride) grown by conventional PECVD (50 nm Si_3N_4 on Si substrate) were examined with this technique. Results indicated a 0.8 eV core level shift in the N $1s$ spectrum for the hot-wire film, relative to the spectrum of the plasma-grown film. These shifts to higher binding energy could be associated with an N-Si$_2$ bond structure[7] (unsaturated bond on N), as opposed to the N-Si$_3$ structure expected of stoichiometric silicon nitride. Larger percentages of oxygen were present in the HWCVD film, suggestive of SiO_2, and an examination of the Si signal yielded a Si/N ratio of approximately 1.3. These results suggest that the film was a combination of SiO_2 and SiN$_x$, possibly a silicon oxynitride ($Si_xO_yN_z$).

FR	Q_S (sccm)	Q_N (sccm)	T (nm)	n
1%	8	8	62	1.8
2%	16	8	128	1.8
4%	32	8	287	1.9
8%	32	4	129	2.5

Table 1. Film growth conditions and results. FR refers to diluted SiH_4 (1% in He)/NH_3 flow rate ratio; Q_S and Q_R refer to SiH_4(1% in He) and NH_3 flow rates in sccm, respectively; T refers to SiN$_x$ film thickness in nm; n refers to film index of refraction

Variation of SiH$_4$/NH$_3$ Flow Ratio
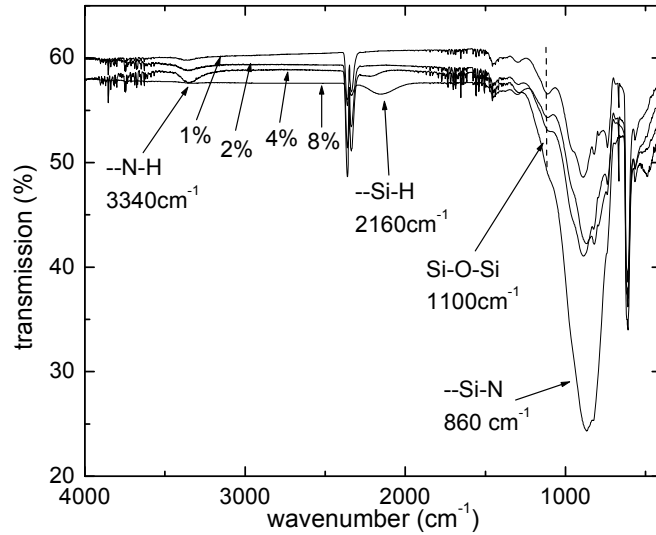
Fig. 1. FTIR transmission spectra of films grown under different SiH$_4$/NH$_3$ flow ratios
(indicated in %).

Prompted by the results indicating that the initial growth conditions led to a film of low
index (1.8), a series of different SiH4/NH3 flow ratios were used to examine the effects
on film properties. The films to be described were grown at a substrate temperature of
300oC for a period of 40 min, with a wire temperature of 1800oC and a total pressure of
100 mTorr. Fig. 1 provides the Fourier Transform Infrared (FTIR) transmission spectra
for a series of four SiNx films grown under different SiH4/NH3 flow ratios: 1, 2, 4, and
8%. Table 1 provides the flow rates used for film growth (FR = flow ratio, QS = SiH4
mixture flow rate, QN = NH3 flow rate), as well as the resulting film thickness ('t') and
refractive index ('n'). Peak assignments were based on data by Lanford and Rand2. The
most prominent feature in the transmission spectra is the Si-N absorption around 860 cm-
1; the breadth of this feature suggests that the SiNx films are
amorphous. The features at 2160 cm-1 and 3340 cm-1 were assigned to Si-H and N-H
stretches, respectively. Evident from Fig. 1 also is that the majority of H is bound to N
for the 1, 2, and 4% flow ratios and there is an abrupt transition at 8%, at which point H
becomes mostly bound to Si. For the 1, 2, and 4% cases, it is likely that the H observed
comes from NH2 species produced at the wire. For the 8% case, the H of the film likely
results from atomic H (produced by SiH4 decomposition) passivating Si dangling bonds
present in the growing film. Using absorption cross sections provided by Lanford and
Rand2, an estimate of the hydrogen concentration in the various films could be obtained.
The range of values obtained by this method was 0.9-1.5x1022cm-3, although the degree
of uncertainty associated with these measurements prevents the emergence of a clear
trend in hydrogen content with respect to flow ratio. Other trends are noticeable from
Table 1. The growth rate is proportional to the product of the SiH4 and NH3 flow rates.

Also, the refractive index increases from 1.8 up to 2.5, with the 4% flow ratio film being the closest to stoichiometric silicon nitride (2.0). Finally, Fig. 1 reveals that the 1% film has a prominent Si-O-Si feature that is diminished or absent in films grown at higher flow ratios.

Rutherford Back Scattering and Hydrogen Forward Scattering Analysis

To complement these FTIR measurements, Rutherford Backscattering (RBS) and Hydrogen Forward Scattering (HFS) measurements were made to determine the stoichiometry and hydrogen content of a select number of SiN_x films. The films chosen for analysis were the 1% and 8% flow ratio films, in addition to two films grown at a flow ratio of 6% (all other conditions identical), one of which was subjected to a post-deposition H_2 treatment; FTIR analysis of the 6% flow ratio films revealed that H was bonded predominantly to Si, as in the 8% case. The post-deposition H_2 treatment was carried out under conditions identical to SiN_x deposition, but with the replacement of SiH_4 and NH_3 with H2 at the same 100 mTorr total pressure. The rationale for this treatment was to determine whether additional H (produced by H_2 decomposition on the wire) could be incorporated into the as-grown SiN_x.

Table 2 provides a summary of the RBS, HFS, and FTIR film analysis. As expected, the RBS data reveal an increase in the Si/N ratio in the film as the SiH_4/NH_3 flow ratio increases. All values are greater than the value of 0.75 expected of stoichiometric silicon nitride, although the value of ~1 obtained with FR = 1% is attributed to the presence of SiO_2. There is a slight decrease in the Si/N ratio after the post-deposition H_2 treatment, suggesting an etching effect of H on the Si of these Si-rich films. The HFS data reveal that the FTIR method of determining H-content is suitable for approximate determinations, but can be in error by as much as a factor of 2. Also revealed by HFS is an increase in the overall atomic percentage of H as the flow ratio (or Si/N) increases, supporting the idea that SiH_4 is the primary source of this H at these flow ratios.

Interestingly, the post-deposition H_2 treatment appeared to have little effect on the atomic percentage of H in the film, and may only have served to etch the Si-rich film. The films also exhibited a decrease in atomic density (as determined with RBS, using the known film thickness) as the proportion of Si/N increased. The film subjected to the H_2 treatment showed an increase in atomic density, consistent with the idea that H etched excess Si from the film, followed by densification. Finally, it is noteworthy that the 1% film contains a large percentage of oxygen (23%), while it is absent (within detection limits) in films grown at higher flow ratios. This result is consistent with the earlier FTIR measurements showing a prominent Si-O-Si feature in the 1% film. It has also been observed by Stannowski et al.[4], using similar techniques, that nitride films deposited with a small flow ratio of SiH_4/NH_3 (<2%) undergo post-deposition oxidation, likely due to absorption of H_2O molecules. The authors infer that films grown under these conditions must be porous to allow for H_2O absorption.

Annealing of Hydrogenated SiN_x

For applications where hydrogenated SiN_x is to be used as a passivation coating, the mobility of bound hydrogen is critical as it is thought that the degree of passivation (as measured in minority carrier lifetime) depends the amount of hydrogen released from the

SiN$_x$ film[8]. As a means to study hydrogen release from SiN$_x$, two of the films described previously were chosen. In order to observe the effects of H release from N versus Si, the 2% and 8% flow ratio films were selected. By analogy with the study by Yelundur[8], we chose to anneal each of these films for 5 minutes at temperatures of 400°C, 600°C and 800°C. Between each anneal, the sample was allowed to cool to room temperature, after which FTIR measurements were made to monitor to release of H from the SiN$_x$ film.

Table 2. Summary and comparison of RBS, HFS, FTIR film analysis

Flow Rate Ratio	Film thickness (nm)	Index n	Si/N Ratio (RBS)	Bonded H Concentrat'n (cm^{-3}) (FTIR)	Total H Concentrat'n [H](cm^{-3})/(at. %) (RBS-FS)	Atomic Density (at/cc) (RBS)	Oxygen Concentr'n (at. %) (RBS)
1%	62	1.8	0.99	1.1x10^{22}	0.77x10^{22} / 9.3%	8.2x10^{22}	23%
6%	209	2.2	1.3	0.94x10^{22}	1.2x10^{22} / 16%	7.5x10^{22}	0%
6% +H$_2$	185	2.1	1.1	0.68x10^{22}	1.3x10^{22} / 16%	8.4x10^{22}	0%
8%	129	2.5	2.2	1.5x10^{22}	1.1x10^{22} / 18%	6.2x10^{22}	0%

Figure 2 shows the FTIR spectra at the various annealing temperatures for each of these films, along with an estimate of the H concentration, determined by the aforementioned method and Lanford and Rand[2]. Fig. 2a shows a steady reduction in the H bonded to N as the anneal temperature is increased, with an overall reduction of 70% after the 800°C anneal. Fig. 2b reveals only a slight reduction in the H bound to Si up to 600°C, with a drastic reduction of 80% after the 800°C anneal. These results are in qualitative agreement with results and a H loss mechanism proposed by Boehme et al.[9].

The dominant loss mechanism for H in N-rich films (all H bonded to N) is suggested to be one involving dissociation of Si-N and N-H bonds to form NH$_3$, which may then diffuse through the SiN$_x$ network; this reaction is calculated to be downhill in energy by 0.43 eV. We also observed only a slight decay in the H bonded to Si for annealing temperatures up to 600°C, followed by a rapid decay in Si-H for higher temperatures. Such results suggest a hydrogen loss reaction having a high activation energy (as compared with N-H loss) that is also highly exothermic (considering the rapid decay upon crossing this threshold temperature). Some of the reactions proposed that would satisfy the latter criteria involve: 1) dissociation of Si-H and N-H to form H$_2$ and Si-N, $\Delta E = -1.86$ eV (unlikely due to negligible amounts of N-H in the Si-rich film), 2) recombination of Si-H to form H$_2$ and Si-Si, $\Delta E = -0.49$ eV, and 3) reactions involving larger numbers of Si-H that are increasingly exothermic, forming SiH$_4$ ($\Delta E = -0.52$ eV) and Si$_2$H$_6$ ($\Delta E = -3.6$ eV) as by-products.

2. Solar Cell and Si Defect Passivation with HWCVD Silicon Nitride

In this section, we describe results of research performed under the subcontract connecting the growth and hydrogen content of HWCVD silicon nitride films to defect passivation in Si and in Si solar cells. First, the stoichiometry and hydrogen content of hot-wire CVD-grown silicon nitride was examined as a function of SiH_4/NH_3 flow ratio. Then, the effect of post-deposition hydrogenation treatment on overall film hydrogen content was determined. The hydrogen release properties in Si-rich and N-rich nitride layers were characterized by annealing treatments. Hot-wire nitride layers were deposited onto Evergreen Solar diffused emitter String Ribbon silicon solar cells, and such passivation resulted in cells with comparable J_{SC}, V_{OC}, FF, and efficiency to those fabricated using plasma CVD nitride layers. Defect hydrogenation in Si was studied using attenuated total reflectance FTIR spectroscopy on platinum-diffused silicon substrates, in collaboration with Lehigh University.

Silicon Nitride Passivation

Silicon nitride acts as an effective anti-reflection (AR) coating for solar cells due to its high refractive index, tunable in the range from 1.8-2.5. These films may also serve as passivation coatings for surface and bulk defects in the underlying silicon, due to the large fraction of hydrogen that may be incorporated (up to 25 atomic %).[2] The conventional means for depositing silicon nitride films uses plasma enhanced chemical vapor deposition (PECVD). Another promising technique for low temperature SiN_x growth is hot-wire CVD (HWCVD), also known as catalytic CVD (Cat-CVD).[10] As compared with PECVD, HWCVD offers the advantages of high deposition rate,[10] as the process can take place at pressures higher than those at which a plasma can be sustained. In addition, it has been demonstrated that the process is compatible with large area deposition by careful design of gas delivery and filament geometry.[11] The deposition of high hydrogen content nitride films by HWCVD for photovoltaic applications has been recently demonstrated.[12,13]

Emitter Passivation

Experiments

The system used in the deposition of SiN_x is a high vacuum chamber with a base pressure of order 10^{-9} Torr. Source gases, consisting of SiH_4 (diluted to 1% in He) and NH_3 are introduced through a gas inlet and decomposed on a W wire (0.5 mm dia, 12 cm length, 1800°C temperature). Flow rates of the various gases range from 4-48 sccm, with SiH_4/NH_3 ratios ranging from 1-8%, and pressures in the range of 20-100 mTorr (higher pressures are possible, but were not explored in this study). Under these conditions, growth rates range from 16-52 Å/min, limited largely by the use of dilute SiH_4; rates of up to 0.14 μm/min have been demonstrated with the use of pure SiH_4 and NH_3 ambients.[13] A substrate heater is located approximately 5 cm from the wire, and a shutter is used to protect substrates from the evaporation of impurities from the wire during its initial heating; growth temperatures were approximately 300°C for this study. The substrates used were lightly-doped p-type (350 Ω-cm), double-side polished, float-zone Si, except where otherwise indicated.

Results

A series of different SiH_4/NH_3 flow ratios (FR) were used to examine the effects on film properties. The films to be described were grown at a substrate temperature of 300^oC for a period of 40 min, with a wire temperature of 1800^oC and a total pressure of 100 mTorr. Fig. 1 provides the Fourier Transform Infrared (FTIR) transmission spectra for a series of four SiN_x films grown under SiH_4/NH_3 flow ratios of 1, 2, 4, and 8%. The most prominent feature in the transmission spectrum is the Si-N absorption around 860 cm^{-1}. Also evident from Fig. 1 is that the majority of H is bound to N for the 1, 2, and 4% flow ratios, while at 8%, H is mostly bound to Si. The refractive index, as determined by single wavelength (633 nm) ellipsometry, increases from 1.8 up to 2.5, with the 4% flow ratio film being the closest to stoichiometric silicon nitride (n = 2.0). To complement these FTIR measurements, Rutherford Backscattering (RBS) and Hydrogen Forward Scattering (HFS) measurements were made to determine the stoichiometry and hydrogen content of a select number of SiN_x films. The films chosen for analysis were the 1% and 8% flow ratio films, in addition to two films grown at a flow ratio of 6% (all other conditions identical)[†], one of which was subjected to a post-deposition H_2 treatment. The post-deposition H_2 treatment was carried out under conditions identical to SiN_x deposition, but with the replacement of SiH_4 and NH_3 with H_2 at the same 100 mTorr total pressure. As expected, an increase in the Si/N ratio in the film was observed as the SiH_4/NH_3 flow ratio increased. All values are greater than the value of 0.75 expected of stoichiometric silicon nitride, although the value of ~1 obtained with FR = 1% is attributed to the presence of SiO_2. There is a slight decrease in the Si/N ratio after the post-deposition H_2 treatment, suggesting an etching effect of H on the Si of these Si-rich nitride layers. Also revealed by HFS is an increase in the overall atomic percentage of H as the flow ratio (or Si/N) increases, supporting the idea that SiH_4 is the primary source of this H at these flow ratios. It is noteworthy that the 1% film contained a large percentage of oxygen (23%), while it was absent in films grown at higher flow ratios. This has been attributed to post-deposition absorption of water by the nitride film.[4]

[†]FTIR analysis of the 6% flow ratio films revealed that H was bonded predominantly to Si, as in the 8% case.

For applications where hydrogenated SiN_x is to be used as a passivation coating, the mobility of bound hydrogen is critical as it is thought that the degree of passivation (as measured in minority carrier lifetime) depends the amount of hydrogen released from the SiN_x film.[8] As a means to study hydrogen release from SiN_x, two of the films described previously were chosen. In order to observe the effects of H release from N versus Si, the 2% and 8% flow ratio films were selected. Each film was annealed for 5 minutes at temperatures of 400°C, 600°C, and 800°C. Between each anneal, the sample was allowed to cool to room temperature, after which FTIR measurements were made to monitor to release of H from the SiN_x film. Fig. 2 shows the FTIR spectra at the various annealing temperatures for the 8% (Si-rich) film, along with an estimate of the H concentration, determined by the use of absorption cross sections.[2] This figure reveals only a slight reduction in the H bound to Si up to 600°C, with a total reduction of 80% after the 800°C anneal. For the 2% (N-rich) film, a steady reduction in the H bonded to N is seen as the anneal temperature is increased, with an overall reduction of 70% after the 800°C anneal.
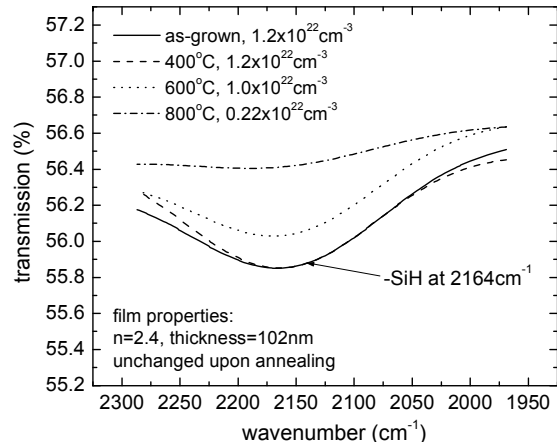
Fig. 2. FTIR spectrum at various annealing temperatures for a film grown with 8% SiH_4 in NH_3; annealing times of 5 min were used.

This difference in hydrogen release kinetics can have important implications for the choice of annealing treatments (temperature, time).

To evaluate the quality of hot-wire-deposited silicon nitride layers relative to their plasma CVD counterparts, films were deposited onto String Ribbon substrates provided by *Evergreen Solar* (Marlboro, MA). Film growth conditions were 3% SiH_4/NH_3 at a total pressure of 70 mTorr for a growth period of 1 hour. The hydrogen content was estimated to be, at minimum, 10 at.% by comparison with previously grown films. The samples were p-type (resistivity of 3 Ω-cm), with a thin phosphorous-diffused n-type layer on top. Due to the large area of the substrates (15 cm x 8 cm), a filament array had to be used to improve thickness uniformity, as shown in Fig. 4. It has been observed[11] that if the filament spacing is at most half the filament-to-substrate distance, then non-uniformity associated with the filament array is eliminated. With this design criterion in mind, the filaments were spaced 2 cm apart, with a wire-to-substrate separation of 5 cm. Samples grown using this wire array exhibited a thickness variation of approximately 15 nm from the center to edge.

Three nitride samples with an average center thickness of 83 nm were chosen for subsequent processing by *Evergreen Solar*. The nitrided samples had a thick aluminum layer deposited on back by a screen-printing process using a commercially available aluminum paste. The samples were then annealed in a belt furnace to form the back contact as well as release H from the nitride layer. Upon fabricating front contacts, the cell's electrical properties were measured. Table 3 provides the short circuit current density (JSC), open circuit voltage (VOC), fill-factor (FF), and efficiency for a

representative hot-wire (HW) nitride cell versus a similarly processed plasma nitride cell produced by Evergreen. The hot-wire nitride cell is comparable in electrical properties (with the exception of JSC) to the plasma nitride cell. Further improvements in JSC might be expected with the use of more uniform nitride coatings.

Table 3. Comparison of electrical properties for hot-wire versus plasma nitride cells.

Cell type	J_{SC} (mA/cm^2)	V_{OC} (mV)	FF	Efficiency (%)
HW nitride	29.99	579	0.712	12.4
Plasma nitride	30.92	584	0.709	12.8

Pt-H Complex Formation

Although it is clear that large fractions of hydrogen can be liberated from nitride films upon annealing, questions remain about whether this hydrogen is simply released into the environment or is driven into the bulk c-Si beneath.

To investigate this issue, the technique of Attenuated Total Reflectance FTIR (ATR-FTIR) was used, which provides for a longer absorption path length that can enable trace vibrational features to be resolved.   The first sample analyzed consisted of a Pt-diffused (to 10^{17}cm^{-3}) p-Si ([B] = $2x10^{15}$ cm^{-3}) ATR prism, onto which a SiN$_x$ film of 80 nm (n = 2.3, Si-rich) was deposited. Pt was chosen given that it is a representative transition metal impurity that acts as a sink for H, and the resulting Pt-H complexes have been well studied, with their vibrational features assigned.[14]   Figure 3 shows the FTIR spectra at various annealing temperatures (10 min anneal) for Pt-H and Si-H (from the nitride layer). Pt-H features are not observed until a temperature of 500°C, consistent with the H-desorption kinetics previously observed for the nitride film. Previous calibration[14] of the Pt-H line
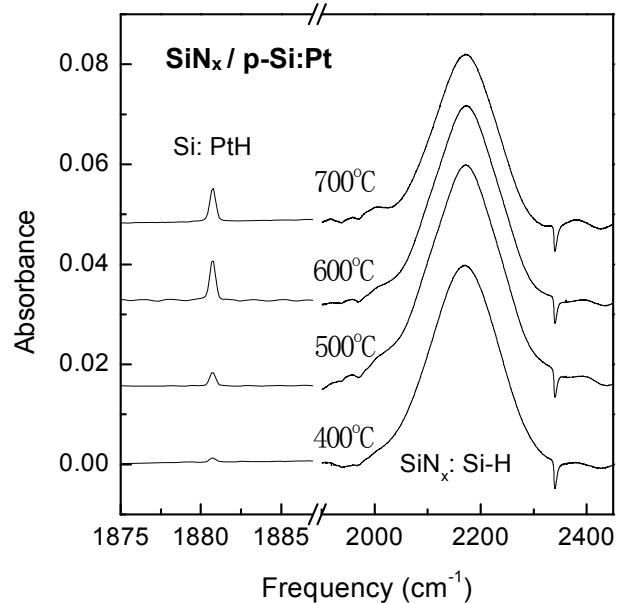
Fig. 3. Creation of Pt-H complexes in bulk Si by annealing of hydrogenated SiN$_x$ layer; annealing times of 10 min were used.

intensities enable an estimate of the concentration of H introduced into the bulk Si. For the 700°C anneal, [Pt-H] is estimated to be 5×10^{12} cm^{-2}. Through successive thinning of this sample to monitor H introduction, the Pt-H concentration is found to drop to 3.1×10^{12} cm^{-2} at a depth of 390 μm. This, in turn, leads to a bulk Pt-H concentration of 5×10^{13} cm^{-3}. Assuming a uniform distribution of H throughout the sample, a hydrogenated layer thickness of 1.1 mm is calculated. A similar Pt-diffused n-type ([P] = 3×10^{16} cm^{-3})
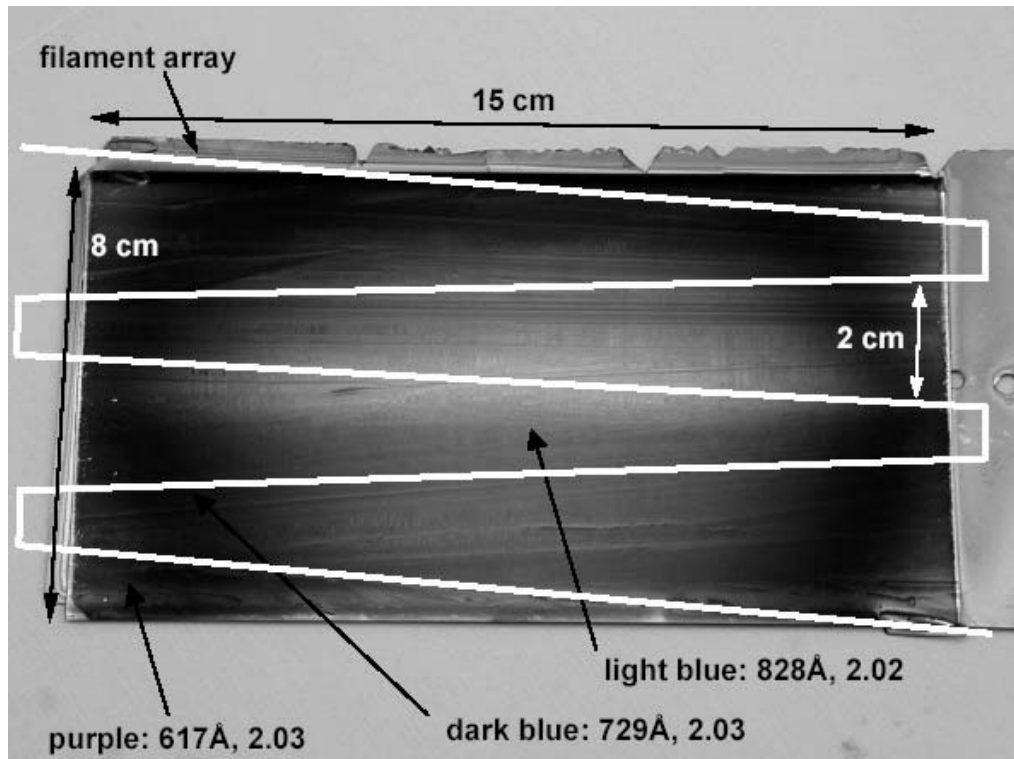
Fig. 4. Photomicrograph of silicon nitride-passivated String Ribbon solar cell; white line depicts position of the wire array during hot wire CVD growth

sample revealed a comparable Pt-H concentration. Two undiffused samples (n, p) were also analyzed, revealing no vacancy-H or dopant-H complexes; both diffused samples also did not reveal such complexes.

Summary of Defect and Emitter Passivation

Varying the SiH$_4$/NH$_3$ ratio from 1-8% produced silicon nitride films ranging in refractive index from 1.8-2.5, with hydrogen content ranging from 9-18 atomic %. Transmission measurements using FTIR revealed a transition in the bonding of H (N-H to Si-H) as the flow ratio was increased beyond 6% SiH$_4$/NH$_3$. Annealing studies revealed different kinetics for H release from Si versus N. String Ribbon silicon cells produced with hot-wire-grown silicon nitride layers show comparable electrical

properties to those produced with plasma nitride layers. The appearance of Pt-H complexes (~10^{14} cm^{-3}) was observed in Pt-diffused Si samples at annealing temperatures consistent with H-release from the nitride top layer

3. Thin Film Silicon Passivation in HWCVD Growth

Overview of Thin Film Si by HWCVD

HWCVD epitaxial growth on large-grained templates is one strategy for the fast, low-temperature growth of large-grained films with hydrogen-passivated low-angle grain boundaries. In this section, we detail results under the subcontract on the role gas phase kinetics in HWCVD growth, film microstructural evolution and passivation of polycrystalline thin films in HWCVD growth.

HWCVD Gas Phase Species Characterization

A knowledge of the primary radicals produced on the wire in a hot-wire chemical vapor deposition (HWCVD) reactor is critical to optimization of film microstructure and quality, as well as for modeling gas-phase chemistry. In year 2, we devoted considerable effort to understanding the changes in the catalytic properties of tungsten hot wires with time during operation. Wire catalytic properties were correlated with changes in surface and bulk microstructure in the wire. The results suggest that there are significant changes in the radical species generated by the wire during extended operation relative to those generated by a new wire. This point is of significant practical importance, since it implies that the radical species generated in film growth by hot wire chemical vapor deposition are a strong function of the frequency with which the wire is replaced (due to breakage or routine service operation).

The following findings resulted from our activities in this area:

- With the use of a new wire, Si is found to be the predominant radical produced in a HWCVD reactor for wire temperatures in excess of 1500 K.
- For temperatures below 1500 K, the SiH$_3$ radical becomes predominant. The small activation energy (8 kcal/mole) observed for SiH$_3$ formation suggests the process is catalyzed with the use of these wires. These results are in qualitative agreement with previous studies of radical chemistry at the wire.
- Radical measurements performed on aged wires show high temperature activation energies for all SiH$_x$ species, suggesting a non-catalyzed process for radical formation.
- Scanning electron microscopy of aged wires revealed a surface both rougher and more irregular than seen with new or heat-treated wires; this morphology is thought to be characteristic of Si deposition (either as free Si or a silicide).
- Auger electron spectroscopy revealed surface Si concentrations as high as 15%, suggesting a two-phase equilibrium between W$_5$Si$_3$ and W (at a Si solubility of 4%). Concentrations of Si in the interior of the wire (2-5%) are of order the solubility limit and reveal that Si diffusion into the wire is significant.

- Radical measurements added further evidence of Si diffusion, as Si was detected in a silane-free ambient following an aging treatment.
- Examining rates for various surface kinetic processes reveals that bulk diffusion of Si through a silicide is the slowest, followed by Si evaporation and then surface decomposition.
- The high rate of surface decomposition supports the idea that Si is in fact the predominant evaporating and diffusing species in and on the wire. In light of the low rate of diffusion through the silicide, the diffusion mechanism in the initial stages of SiH4 exposure must either consist of bulk diffusion through elemental W or large cracks that develop on the wire surface and propagate to the interior.
- Finally, experimentally observed evaporation kinetics suggest that Si desorption from a new wire comes from direct Si-W bond breakage, as opposed to evaporation from Si.

Rates for Surface Kinetic Processes

A comparison of the relative rates for the various surface kinetic processes on the wire, namely, diffusion, evaporation, and decomposition allows further insight into the nature of the wire aging process. At the highest temperatures investigated in this study (~ 2400 K), the solid solubility of Si in W is a few atomic percent, dropping to less than 1 at.% at the lowest temperature (1273 K). To our knowledge, there have been no studies that examined the diffusion of Si into elemental W. A study by Kharatyan *et al.*, however, investigated the diffusion of Si into various silicides of tungsten and molybdenum. For the diffusion of Si into W5Si3 (the only silicide for which data were available), a diffusion coefficient of

$$D_{W_5Si_3}^{Si} = 6.9\exp(-69000 \pm 5000/RT), cm^2/s$$

was obtained. Using this diffusion coefficient, the rate for diffusion (using the wire radius as a lower limit for the characteristic length) as a function of wire temperature is given in Fig. 5.

Data on the evaporation rate of Si from W were unavailable, but the study by Ehrlich does provide an evaporation rate for H from W, which is relevant to the SiH4 decomposition process; this rate is plotted in Fig. 5. The evaporation rate of Si from liquid Si could be determined from the vapor pressure data of Margrave. As liquid Si can form at some point during the aging process (T = 2000°C, W<33%/Si>66%), this rate has relevance to the aged wires of this study. This rate of evaporation, as a function of wire temperature, is also plotted in Fig. 5. Finally, rates of SiH4 decomposition on W were not directly available, but a study by Yang *et al.*[24] suggests the timescale for Si-H bond breaking is of order a few picoseconds (in a liquid environment), establishing a lower bound to the decomposition rate for the significantly higher temperatures in the present study; this rate is included for comparison in Fig. 5.

Examining these rates in Fig. 5, bulk diffusion of Si through the silicide is clearly the slowest process, followed by Si evaporation, and then decomposition. These rates, coupled with experimental observations, give a picture of the relative rates of surface kinetic processes on the wire. First, the high rate of decomposition compared with

evaporation and diffusion suggests that for the vast majority of wire temperatures, Si (as opposed to other SiH_x) is the predominant evaporating/diffusing species; radical measurements in particular support the idea that it is the dominant evaporating species.

At sufficiently low temperatures, however, this process becomes decomposition-limited, and a spectrum of other species is observed. The Auger and radical measurements described earlier provide clear evidence that diffusion through the wire is occurring, and at rates faster than would be predicted by bulk diffusion (through a silicide) alone. This suggests that the majority of Si that diffuses into the wire does so before a thick silicide has formed. Whether this higher *effective* diffusivity is due to a higher intrinsic rate of Si diffusion into W (rather than W_5Si_3) or diffusion occurring primarily through cracks that develop on the surface of the wire is unclear.
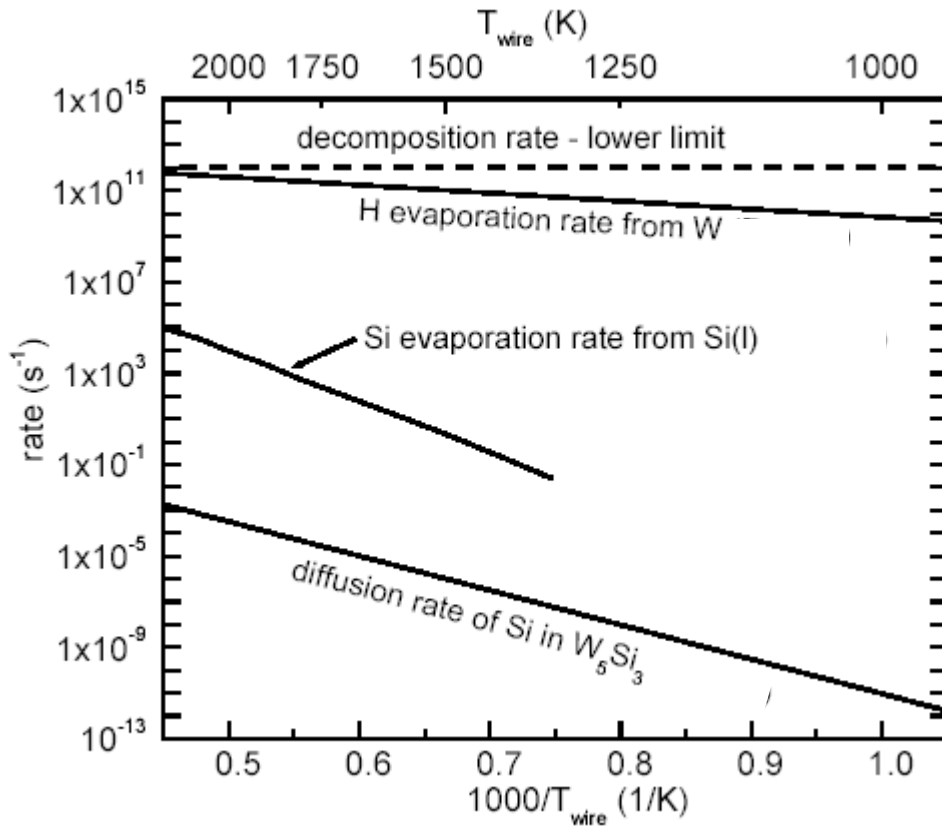
Fig. 5. Rates of interest for wire surface kinetic processes.

Finally, it appears that the rate of evaporation of Si from Si(l) is several orders of magnitude below that of decomposition, even at the highest wire temperatures. It was previously observed, however, that for wire temperatures in excess of 2000 K, a saturation in the Si signal occurs with the use of a new wire that does not occur with an aged wire. This observation is consistent with a competition between evaporation (of Si and/or SiH_4) and decomposition. This, in turn, may suggest that the mechanism of Si desorption from a new wire does not consist of Si evaporation from Si(l), but a different mechanism, namely, the direct desorption of Si from a W surface. The rate for this

process is likely to be of a similar magnitude as H evaporation from W, depicted in Fig. 5. It is also possible that the rate of SiH_4 evaporation becomes comparable to its rate of decomposition at high temperatures, explaining the Si saturation.

A picture then emerges of the hot-wire CVD decomposition process. First, SiH_4 is adsorbed and then rapidly decomposed to Si and H on the surface of a new wire. This surface Si will then either evaporate or, if the surface concentration is high enough, diffuse to the interior of the wire up to its solubility limit. Once the thermodynamic solubility has been reached, excess Si can contribute to the formation of the W_5Si_3 phase, or at higher concentrations, WSi_2. At the highest Si concentrations (> 67%), liquid Si can form at the surface and then Si evaporation from Si(l) becomes the dominant mechanism of Si production. The observation that a new wire readily absorbs Si, but retains it for a long period of time can be explained as a silicide diffusion-limited process. The silicide that forms at the surface acts as a diffusion barrier to Si in the interior of the wire (as well as to further diffusion of surface Si into the wire), and Fig. 5 shows that the characteristic diffusion time at the wire temperature used (~ 1750 C) is, at minimum, several hours.

A Phase Diagram for Morphology and Properties of Low Temperature Deposited Polycrystalline Silicon Grown by Hot-wire Chemical Vapor Deposition

The fabrication of low temperature polycrystalline silicon with internal surface passivation and with lifetimes close to single crystalline silicon is a promising direction for thin film polycrystalline silicon photovoltaics. To achieve high lifetimes, large grains with passivated low-angle grain boundaries and intragranular defects are required. We investigate the low-temperature (300-475°C) growth of thin silicon films by hot-wire chemical vapor deposition (HWCVD) on Si (100) substrates and on large-grained polycrystalline silicon template layers formed by selective nucleation and solid phase epitaxy (SNSPE). Phase diagrams for dilute silane deposition varying substrate temperature and for pure silane varying hydrogen dilution are shown. We will discuss the relationship between the microstructure and photoconductive decay lifetimes of these undoped layers on Si (100) and SNSPE templates as well as their suitability for use in thin-film photovoltaic applications.

HWCVD epitaxial growth on large-grained templates is one strategy for the fast low-temperature growth of large-grained films with hydrogen-passivated low-angle grain boundaries. We propose a structure by which a template with grains on the order of 10–100 μm is fabricated on ITO-coated glass or another low cost conductive substrate by a solid-phase crystallization process called SNSPE[15]. This layer serves as the n+ back surface field, and the n and p+ layers are grown epitaxially on this template by HWCVD, using phosphine and tri-methyl boron as dopants. In order to achieve this goal, investigation of the phase diagrams that lead to epitaxial growth in HWCVD are necessary. Preliminary work towards the fabrication of this cell and the necessary intermediate goals are discussed.

Dilute Silane Growth

In order to promote crystalline growth under dilute silane conditions, we used a high hydrogen partial pressure dilution ratio of 50:1, using a mixture of 4% SiH_4 in He at a partial pressure of 25 mTorr and H_2 at a partial pressure of 50 mTorr. The 0.5mm diameter tungsten wire was positioned 2.5 cm from the substrate for a growth rate of 1Å/s. The wire temperature was set to $1800^{\circ}C$ as measured by optical pyrometry, and substrate temperatures ranged from $300^{\circ}C$ to $475^{\circ}C$.

Silicon (100) substrates and large-grained polycrystalline layers formed by SNSPE were used as templates for epitaxial growth. The formation of the large-grained templates is described in the Chen PhD thesis [15]. The resulting polycrystalline templates have grain sizes on the order of 10 to 100 μm with low-angle grain boundaries. Before growth, both surfaces were cleaned with UV ozone for 10 minutes followed by an HF dip. Once in the chamber, they are heated at $200^{\circ}C$ at a pressure of less than 10^{-6} Torr to desorb any residual hydrocarbons.

Pure Silane Growth

Using pure silane, the influence of dilution ratio was studied. The substrate temperature was held constant at $380^{\circ}C$ while graphite filaments set to $2100^{\circ}C$ by optical pyrometry were placed 3.5 cm from the substrate. The H_2 to SiH_4 ratio ranged from 10 to 50, total pressure also had to be adjusted for the higher H_2 flow rates and ranged from 20 to 50 mTorr. Substrates were cleaned as described above.

Dilute Silane Growth - Substrate Temperature Effects

We used TEM and RHEED to characterize the crystallinity of films grown at 50:1 hydrogen dilution and temperatures between $300\text{-}475^0C$ in the 50 nm to 2 μm thickness regime and observed four phases of growth. A completely defect-free epitaxial phase was observable by TEM at thicknesses below 50nm; the twinned epitaxial, mixed and polycrystalline phases were observable by TEM and RHEED[16]. Twinned epitaxial silicon denotes silicon material containing twin boundaries, but no other dislocation or grain boundary defects. From this data, we derived the phase diagram in Fig. 6. At 300^0C, the predominant phases are epitaxial and twinned, with a transition to mixed phase or polycrystalline growth occurring somewhere between 1-2 μm of growth. As temperature increases, the epitaxial and twinned phases no longer persist and the transition to mixed phase or polycrystalline growth occurs at smaller film thicknesses. This is in direct contrast to work done by Thiesen[17] and Watahiki[18] where epitaxial thickness increased with substrate temperature. We believe that the decrease in epitaxial thickness with the increase in substrate temperature is due to an interplay between surface hydrogenation at low temperatures and surface oxidation at high temperatures that reduces the epitaxial thickness. This is possibly related to the higher hydrogen content in HWCVD as compared to PECVD or MBE along with oxygen contamination in the deposition chamber[19].
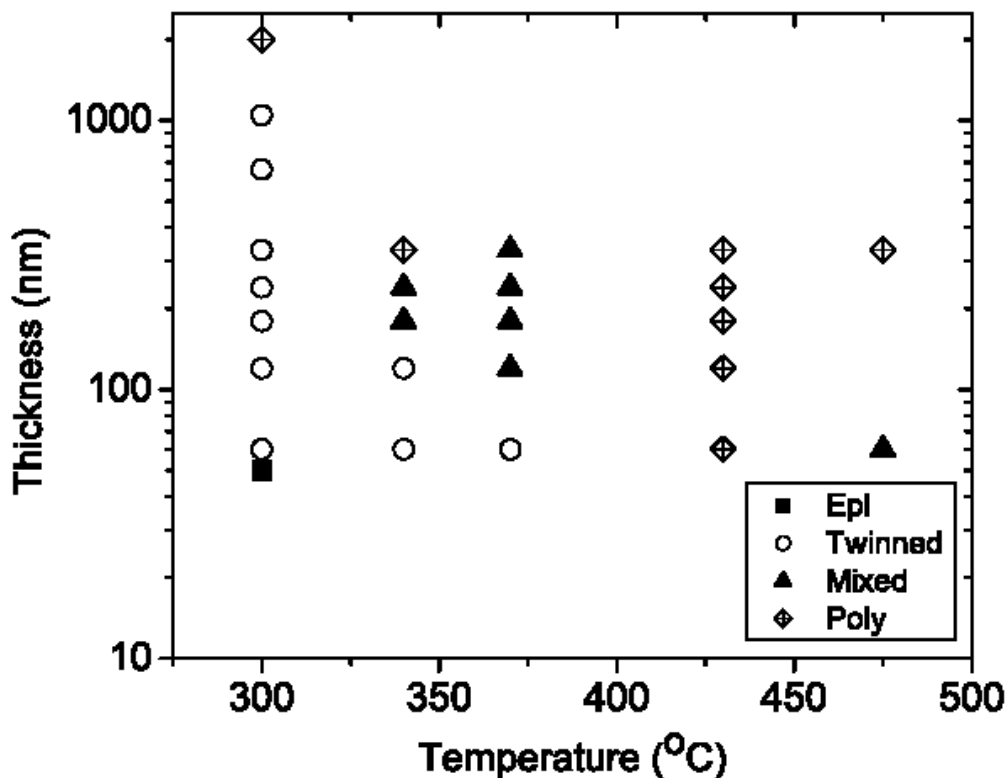
Fig. 6: Phase diagram of HWCVD films grown at 50:1 hydrogen dilution with 4% SiH$_4$ in He.

Silicon films 300 nm thick grown on SNSPE templates under the same conditions showed epitaxial growth results consistent with local low temperature epitaxy on each of the 100 μm grains in the SNSPE templates, as shown in Fig. 7. Epitaxial breakdown is observed in the diffraction pattern of the HWCVD film, but some of the underlying low-order diffraction spots are visible. The underlying film therefore likely has morphology similar to that of the HWCVD films on Si(100). The effect of the orientation of the underlying grain structure of the SNSPE template on the morphology of the HWCVD film is shown in Figure 7.

Cross-sectional analysis of these films reveals some areas of epitaxial growth as well as some areas of columnar growth. Before HWCVD growth, the SNSPE templates were cleaned in a solution of 3:7 HNO$_3$: H$_2$O, which has been shown by Auger spectroscopy to remove elemental Ni from the template surface[20]. The lack of epitaxy in some areas is thus more likely to have been caused by the presence of ubiquitous surface contaminants, such as carbon and oxygen, than by nickel nanoparticles, since a similar microstructure can be seen in deposition on Si(100) substrates as well.

Pure Silane Growth – Hydrogen Dilution Effects

We used TEM and Raman Spectroscopy to determine the structure of Si thin films grown at 380°C with graphite wires at 2100°C. We found that the crystallinity did not increase with hydrogen dilution as expected[21]. Instead, an amorphous/protocrystalline structure is observed at dilution ratios of 20 to 30, while at both the 40 and 10 H_2/SiH_4 dilution ratios we observe epitaxial growth with polycrystalline breakdown. This suggests a complex interaction between pressure and dilution, which will be discussed later.
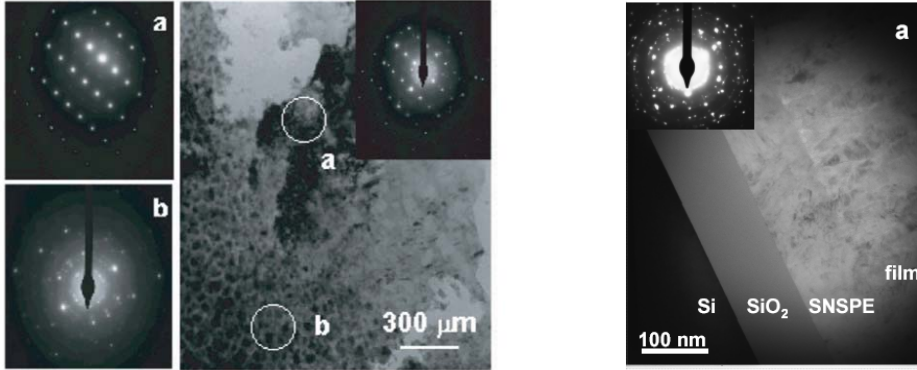
Fig. 7. Plan-view TEM of HWCVD epitaxial film (T=300^0C) on SNSPE template. (a) Selected area diffraction pattern from underlying SNSPE template. (b) Selected area diffraction pattern from HWCVD film on SNSPE template. (c) Bright-field image indicating selected area diffraction regions. Inset: diffraction from entire area. (d) Bright-field image of HWCVD film (T=300^0C) on SNSPE template showing selected area diffraction region. Inset: selected area diffraction pattern showing areas of large-grained polycrystalline growth.

Table 4. Results of HWCVD growth with pure silane at 380 $^\circ$C substrate temperature and at 2100 $^\circ$C graphite filament temperature with 3.5cm spacing.

Hydrogen Dilution Ratio	Pressure (mTorr)	Deposition Rate (nm/min)	Raman Crystallinity %	Phase
50:1	50	4	83	Poly
40:1	27	5	84	Epi/poly
30:1	20	3	9	a-Si/Proto
20:1	20	6	10	a-Si/Proto
10:1	20	9	96	Epi/poly

Minority Carrier Lifetimes of HWCVD Films

The minority carrier lifetimes of 1.5–15 μm thick films grown at 300 $^{\circ}$C on Si(100) and SNSPE templates were determined through resonant-coupled photoconductive decay (RCPCD) measurements[22]. These films began with epitaxial growth which broke down to microcrystalline growth at thicknesses between $1 - 2$ μm. Although the microstructure of these films is mostly microcrystalline, the lifetimes are microseconds long. The lifetimes for films on Si(100) range from 5.7 to 14.8 μs while those for films on SNSPE templates range from 5.9 to 19.3 μs under low level injection conditions, as summarized in Figures 8 and 9. Residual nickel present in the SNSPE templates does not significantly affect the lifetime of films grown on SNSPE templates, making the growth of epitaxial layers by HWCVD on SNSPE templates a viable strategy for the fabrication of thin film photovoltaics.
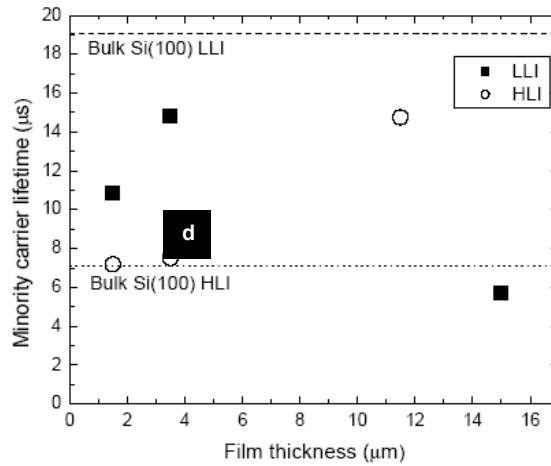

Fig. 8. LLI and HLI minority carrier lifetimes of HWCVD films on Si(100) as measured by RCPCD. The dashed and dotted lines represent the LLI and HLI lifetimes, respectively, of the bulk Si(100) substrate.
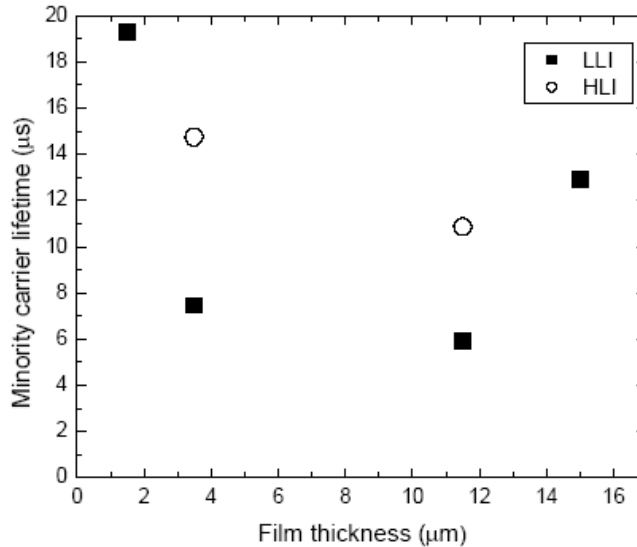

Fig. 9. LLI and HLI minority carrier lifetimes on SNSPE templates.

Hot Wire CVD – A Simple Model

The epitaxial growth and growth breakdown trends for HWCVD growth are consistent with a simple model correlating epitaxial growth breakdown with surface oxidation. Starting with an initial hydrogen surface coverage dependent only on the substrate temperature determined from temperature-programmed desorption data[23], the model determines the steady-state surface hydrogen coverage by balancing thermal desorption of surface hydrogen with adsorption and abstraction of surface hydrogen by atomic hydrogen produced by the hot wire. Oxygen atom can be incorporated into the film at any empty sites. We used the model to determine the amount of oxygen deposited during the growth of the first monolayer of silicon for a given growth temperature as a function of dilution ratio R ($R=H_2/SiH_4$) at constant pressure, assuming that all silicon atoms incident on the substrate contribute to growth.[19]

Figure 10 shows that the maximum silicon to oxygen ratio decreases with temperature for between 311°C and 520°C at a hydrogen dilution ratio of 50:1. This may explain the decrease in epitaxial thickness with temperature in Fig. 6.
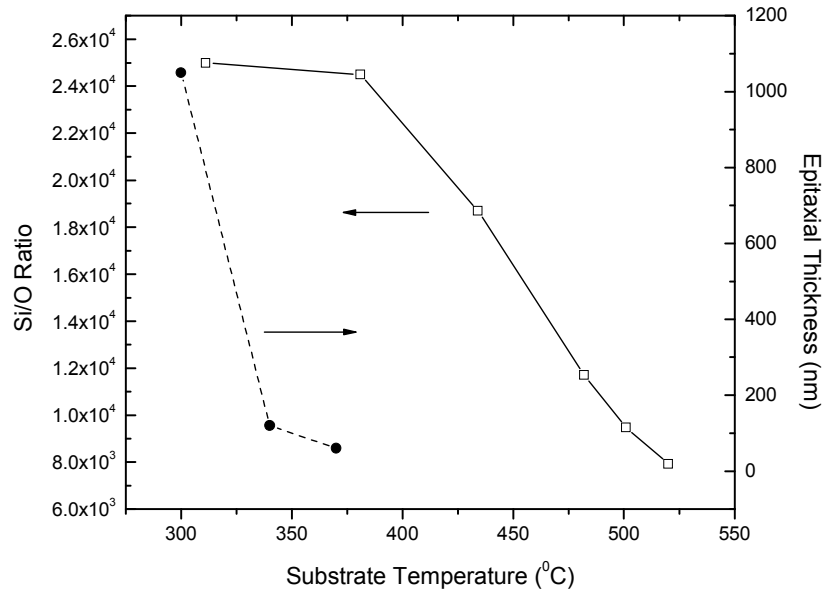
Fig. 10. Silicon to oxygen ratio in the first monolayer of growth as a function of substrate temperature for dilute silane growth at 50:1 hydrogen dilution and epitaxial thickness.

The dependence of the epitaxial thickness on the silicon to oxygen ratio is difficult to quantify. However, it is known that, during MBE crystal growth, impurities at the growing interface can lead to surface roughening and subsequent epitaxial breakdown through the formation of voids which may lead to twinning and surface facets[24]. For our dilute silane experiments, a decrease in the maximum silicon to oxygen deposition ratio with temperature, as predicted by the model, may explain the observed decrease in epitaxial thickness with temperature.

Figure 10 may also give some qualitative insight into the amorphous/protocrystalline peak at intermediate dilution for growth with pure silane. In this simulation the deposition pressure is changed along with the dilution ratio in order to match the deposition conditions in Table 4. The Si/O ratio is highest at the two extremes of the deposition conditions: low dilution ratio, low pressure; and high dilution ratio, high pressure. The high Si/O ratio correlates with a higher degree of crystallinity. A low Si/O ratio leads to the amorphous and ultimately protocrystalline film. Through these experiments and simulations we are working toward determining the optimal deposition parameters for epitaxial growth with polycrystalline breakdown.
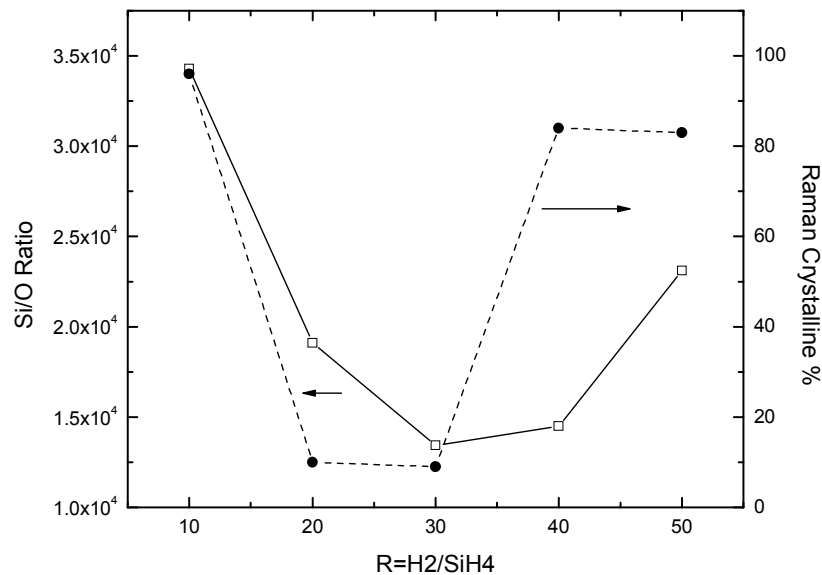
Fig. 11. Silicon to oxygen ratio in the first monolayer of growth as a function of R for pure silane growth using the deposition conditions in Table 4 along with the Raman crystalline %.

We have explored the phase space of HWCVD growth with dilute and pure silane at various substrate temperatures and dilution ratios. The complex interaction between deposition parameters can be qualitatively explained by an oxidation model. Twinned epitaxial growth of Si to thicknesses over 1 μm is observed with polycrystalline breakdown under dilute conditions.

The minority carrier lifetimes of nearly-intrinsic epitaxial/microcrystalline films grown on Si (100) by HWCVD range from 5.7 to 7.5 μs. The lifetimes of films grown under the same conditions on SNSPE templates range from 5.9 to 19.3 μs, making them suitable for incorporation into photovoltaic devices. In particular, residual nickel from the SNSPE templates does not appear to be significantly detrimental to the lifetime of films grown on these templates. If the mobilities in these films are also high, it is possible that

HWCVD epitaxy on large-grained SNSPE templates could be a viable strategy for the fabrication of thin-film photovoltaics.

HWCVD Si Film Passivation

Under this subcontract, we investigated thin film cell structures fabricated on polycrystalline silicon templates with grain sizes on the order of ten microns on glass coated with a transparent, conductive oxide (TCO). Templates were formed by a solid-phase crystallization process called selective nucleation solid phase epitaxy (SNSPE)[15]. The template layer is designed to serve as the n+ layer of the device, and as the epitaxial template for n and p+ layers grown by HWCVD, using phosphine and trimethyl boron as dopants (Fig. 12).   As a simple test structure for the passivation studies, we fabricated, n-type HWCVD Si films on p-type Si(100) substrates, in order to study both the microstructure and electrical properties of the film using a single crystal template, without the complications created by the large-grained polycrystalline template seed layer.
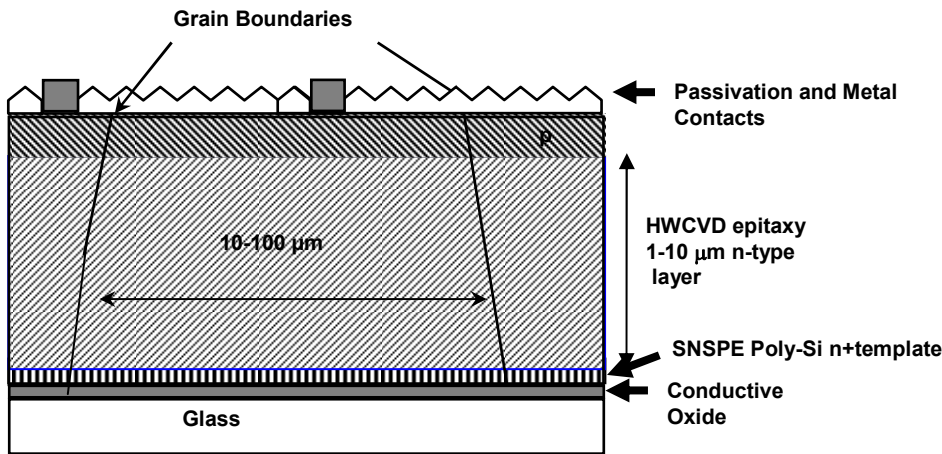
Fig. 12.   Schematic of proposed photovoltaic device incorporating epitaxial Si growth on a large-grained polycrystalline template fabricated by SNSPE.

Microstructure and Passivation Effects on Open Circuit Voltage

Hydrogen-passivated silicon films grown via hot wire chemical vapor deposition (HWCVD) are promising candidates for polycrystalline Si solar cell absorber layers. We studied the correlation of film microstructure and passivation with open-circuit voltage, a key cell electrical characteristic, for varying growth conditions and post-deposition treatments. We examined the role of hydrogen-dilution on growth morphology and Voc. *Importantly, the results indicate effective hydrogen passivation in the 'bulk' of HWCVD-deposited Si films* to the extent that the Voc is highly sensitive to surface passivation. Surface passivation, rather than bulk passivation, is thus identified as the limiting factor in achieving higher Voc; hence we have investigated the effect of several post-deposition passivation treatments on surface passivation. Our goal in this work was to elucidate the role of hydrogen in HWCVD Si film bulk passivation, crystalline fraction, growth

morphology, and its relation to film electrical properties. Varying growth conditions and observing the subsequent effect on microstructure and open-circuit voltage enables us to optimize these characteristics for polycrystalline Si thin film solar cell absorber applications.

In these experiments, silicon films were grown on CZ-grown Si(100) via HWCVD, with either undoped or n-type with phosphine (5% in SiH_4) as the dopant gas, at substrate temperatures varying from 230 C to 350 C. Silane gas (1% in Ar) is diluted with hydrogen in various ratios of $R = H_2/SiH_4$. We used tungsten filaments operated at T~1700 °C to catalyze SiH_4 decomposition. Open circuit voltage measurements were performed for n-type films with phosphorus doping of 1 x 10^{15} cm^{-3} grown on CZ-grown p-type Si (100) with boron doping of 1 x 10^{16} $cm^{-3.}$ Steady-state V_{oc}[25] measurements were performed on unmetallized HWCVD n-Si films/p-Si (100), and growth morphology was observed by cross-sectional transmission electron microscopy.

HWCVD Growth and Morphology

The structure of as a function of hydrogen dilution was investigated by electron microscopy, which reveals an increase in porosity for growth in the range 230 °C < T < 350 °C as dilution is decreased from R = 480 to R = 30, for a total pressure of P = 120 mTorr. The resulting images reveal a more rapid breakdown to a porous microstructure as R decreases, as shown in Fig. 13. The pore-permeated microstructure originates during film growth and pores are oriented perpendicular to the surface. Although films exhibiting this porous microstructure would be suspected to be prone to oxidation, Raman measurements taken after ambient exposure for ~10 weeks did not indicate oxide formation.
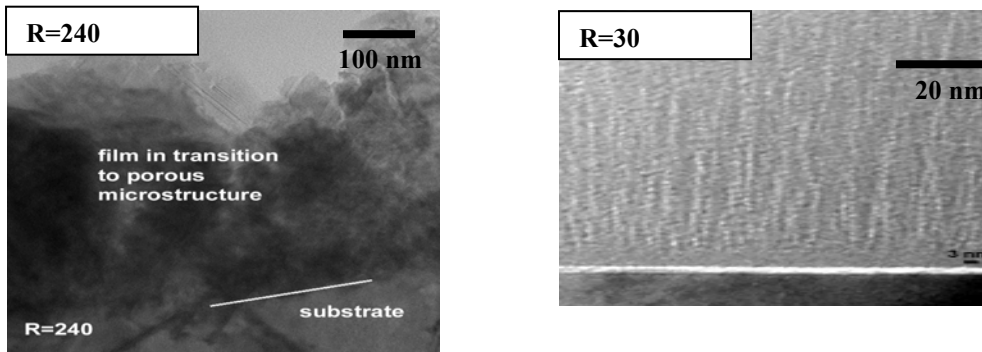
Fig. 13. Cross-sectional TEM of growth morphology at various hydrogen dilutions [26].

Open-Circuit Voltage

An increase in open-circuit voltage with hydrogen dilution is observed for 1000 nm thick films grown with a hydrogen dilution in the range 0 < R < 244, as shown in Fig. 14. For R = 244, an initial V_{oc} of 400 mV was observed, but V_{oc} decreased to 290 mV after one week of ambient exposure. Another set of films 885nm thick were grown with a hydrogen dilution ranging from 45 < R < 180, with a similar increase in V_{oc} observed

with H-dilution. The highest stabilized V_{oc} of 350 mV was observed for 885 nm thick films deposited at R=90. We attribute the higher V_{oc} to lower film porosity compared to films grown at lower dilution, which leads to less surface recombination due to the smaller surface area. As the thickness of the film increases, dense epitaxial growth is observed to transition into a porous microstructure. For this reason, we do not observe a maximum stabilized V_{oc} for the thickest film.

The open-circuit voltage of both the 125 nm and 885 nm films was measured initially and after 1 week in ambient air, and significant changes are observed[27]. The rise in V_{oc} over time in ambient air indicates sufficient passivation of the bulk of the film due to high hydrogen content during growth. We attribute this change in V_{oc} to a change in surface passivation during ambient oxidation, suggesting that hydrogen passivation of defects in the 'bulk' of the film is sufficient to prevent bulk recombination from limiting V_{oc}.
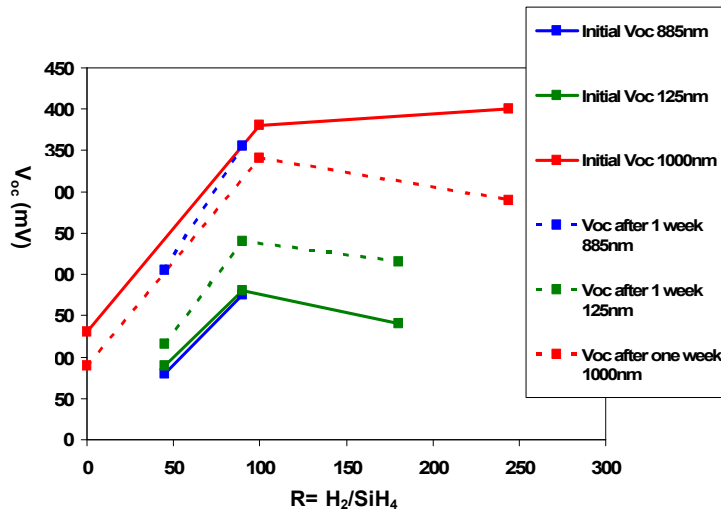
Fig. 14. V_{oc} with hydrogen dilution immediately after deposition and after one week in ambient air.

Surface Passivation

The results of various surface treatments are shown in Fig 15. Annealing at 900 C causes a dramatic decrease in V_{oc} that we attribute to hydrogen evolution from the film. Chemical oxidation by liquid immersion in H_2O: H_2O_2: NH_4OH during an RCA II clean results V_{oc} comparable to those for films that undergo ambient air oxidation.

We investigated the correlation between microstructure and surface passivation on V_{oc} in low temperature HWCVD polycrystalline silicon thin films. Film porosity increases with decreasing hydrogen dilution for films grown under high hydrogen dilution. In general, epitaxial growth and low porosity correlate with higher V_{oc}. Results from post-deposition treatments show promising improvements in V_{oc} with RCA oxidation. A decrease in V_{oc} is seen after high temperature anneals, suggesting loss of bulk hydrogen passivation during high temperature annealing. These results clearly demonstrate the ability to achieve high V_{oc} for well-passivated films, and future work

will address achieving stable passivation for HWCVD Si polycrystalline films with high initial V_{oc}.
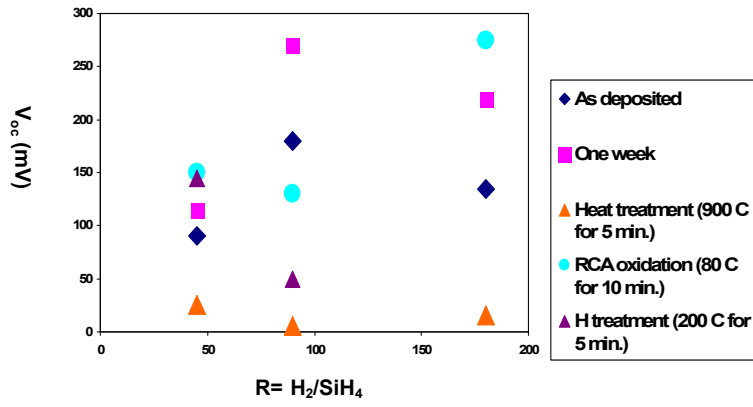
Fig. 15. Open-circuit voltage with hydrogen dilution after various post-deposition treatments.

References

[1] H. Sato, A. Izumi, and H. Matsumura, Appl. Phys. Lett. **77,** 2752 (2000).

[2] W. Lanford and M. Rand, J. Appl. Phys. **49,** 2473 (1978).

[3] H. Matsumura, Jpn. J. Appl. Phys. **37,** 3175-3187 (1998).

[4] B. Stannowski, M. van Veen, and R.E.I. Schropp, Mat. Res. Soc. Symp. Proc. **664,** A17.3.1 (2001).

[5] J. Holt, M. Mason, D. Goodwin, and H. Atwater, unpublished.

[6] R. Sanderson, *Chemical Bonds and Bond Energy* (Academic Press, New York, (1976).

[7] S. Kaluri and D. Hess, Appl. Phys. Lett. **69,** 1053 (1996).

[8] V. Yelundur, A. Rohatgi, A. Ebong, A. Gabor, J. Hanoka, and R. Wallace, J. Electron. Mater. **30,** 526 (2001).

[9] C. Boehme and G. Lucovsky, J. Appl. Phys. **88,** 6055 (2000).

[10] B. Nelson, E. Iwaniczko, A. Mahan, Q. Wang, Y. Xu, R. Crandall, and H. Branz, Thin Solid Films **395,** 292 (2001).

[11] A. Ledermann, U. Weber, C. Mukherjee, and B. Schroeder, Thin Solid Films **395,** 61 (2001).

[12] J. Holt, M. Swiatek, D. Goodwin, and H. Atwater, Mat. Res. Soc. Symp. Proc. **715,** 10.2.1 (2002).

[13] J. Moschner, J. Schmidt, and R. Hezel, 29th IEEE Photovoltaic Specialists Conference, New Orleans, LA (2002).

[14] M. Weinstein, M. Stavola, K. Stavola, S. Uftring, J. Weber, J. Sachse, and H. Lemke, Phys. Rev. B **65,** 035206-1 (2001).

[15] C. M. Chen, "Polycrystalline Silicon Thin Films for Photovoltaics," Ph.D. thesis in Applied Physics, California Institute of Technology, 2001.

[16] M. S. Mason, Christine E. Richardson and Harry A. Atwater, MRS Proceedings A8.11, San Francisco, 2004.

[17] J. Thiesen, E. Iwaniczko, K.M. Jones, A. Mahan, and R. Crandall, Appl. Phys. Letters, vol. 75, pp. 992, 1999.

[18] T. Watahiki, A. Yamasa, and M. Konagai, J. Crys. Growth, vol. 209, pp. 335, 2000.

[19] Christine E. Richardson, M. S. Mason, and Harry A. Atwater Thin Solid Films, to be published.

[20] R.A. Puglisi, H. Tanabe, C.M. Chen, and Harry A. Atwater, Mat. Sci. Eng. B, vol. 73, pp. 212, 2000.

[21] M. S. Mason, "Synthesis of Large-Grained Polycrystalline Silicon by Hot-Wire Chemical Vapor Deposition for Thin Film Photovoltaic Applications," California Institute of Technology, 2004.

[22] R. K. Ahrenkiel and S. Johnston, Sol. Energy Mat. Sol. Cells, vol. 55, pp. 59, 1998.

[23] M.C. Flowers, N. B. H. Jonathon, Y. Liu, and A. Morris, Journal of Chemical Physics, vol. 99, pp. 7038, 1993.

[24] D. J. Eaglesham, Journal of Applied Physics, vol. 77, pp. 3597, 1995.

[25] R.A. Sinton and A. Cuevas, "A Quasi-Steady-State Open-Circuit Voltage Method for Solar Cell Characterization", Proceedings of the 16th European Photovoltaic Solar Energy Conference, Glasgow, United Kingdom (2000).

[26] C. E. Richardson, "Low-Temperature Hot-Wire Chemical Vapor Deposition of Epitaxial Films for Large-Grained Polycrystalline Photovoltaic Devices", Ph. D. Thesis, California Institute of Technology, (2006).

[27] C. E. Richardson, K. Langeland, and H. A. Atwater, "Electronic Properties of Low Temperature Epitaxial Silicon Thin Film Photovoltaic Devices Grown by HWCVD", Proceedings of the 4th International Conference on Hot-Wire CVD Process, Takayama, Japan, (2006).

Personnel Associated with Subcontract
Researchers:
1. Krista Langeland, graduate student
2. Christine E. Richardson, graduate student
3. Maribeth S. Mason, graduate student
4. Jason Holt, graduate student
5. Youngbae Park, postdoctoral research
6. Harry A. Atwater, principal investigator

Collaborators:
1. Andrew Gabor, Evergreen Solar, Inc.
2. David Carlson, BP Solar
3. Michael Stavola, Lehigh University
4. David Goodwin, Caltech
5. William A. Goddard, Caltech
6. Richard Ahrenkiel, NREL

Publications under subcontract

PhD Theses:

1. Jason Knowles Holt, PhD. Chemical Engineering, 2002.
2. Maribeth Swiatek Mason, PhD, Materials Science, 2004.
3. Christine Esber Richardson, PhD, Applied Physics, 2006.

Journal Publications:

1. J.K. Holt, M. Swiatek, D.G. Goodwin, R.P. Muller, W.A. Goddard, III and H.A. Atwater. *Thin Solid Films* 395 (2001), pp. 29–35.

2. "Gas Phase and Surface Kinetic Processes in Polycrystalline Silicon Hot-Wire Chemical Vapor Deposition", J. K. Holt, M. Swiatek, D. G. Goodwin, and H.A. Atwater, *Thin Solid Films* 395, 29-35 (2001).

3. "High Hydrogen Content Silicon Nitride For Photovoltaic Applications Deposited By Hot-Wire Chemical Vapor Deposition", Jason K. Holt, Maribeth Swiatek Mason, David G. Goodwin, and Harry A. Atwater, Mat. Res. Soc. Symp. Proc., Materials Research Society, Pittsburgh, PA, (2002).

•

4. Holt, JK; Swiatek, M; Goodwin, DG; Atwater, HA, The aging of tungsten filaments and its effect on wire surface kinetics in hot-wire chemical vapor deposition, *Journal of Applied Physics*, 92 (8): 4803-4808 OCT 15 2002.

•

5. Mason, MS; Chen, CM; Atwater, HA, Hot-wire chemical vapor deposition for grained polycrystalline epitaxial silicon growth on large-silicon templates, *Thin Solid Films*, 430 (1-2): 54-57 APR 22 2003

6. Jiang, F; Stavola, M; Rohatgi, A; Kim, D; Holt, J; Atwater, H; Kalejs, J, Hydrogenation of Si from SiNx(H) films: Characterization of H introduced into the Si, *Applied Physics Letters*, 83 (5): 931-933 AUG 4 2003

7. Holt, JK; Goodwin, DG; Gabor, AM; Jiang, F; Stavola, M; Atwater, HA, Hot-wire chemical vapor deposition of high hydrogen content silicon nitride for solar cell passivation and anti-reflection coating applications, *Thin Solid Films*, 430 (1-2): 37-40 APR 22 2003

8. Mason, MS; Holt, JK; Atwater, HA, Quantitative modeling of nucleation kinetics in experiments for poly-Si growth on SiO2 by hot wire chemical vapor deposition, *Thin Solid Films*, 458 (1-2): 67-70 JUN 30 2004

9. Mason, MS; Holt, JK; Atwater, HA, Quantitative modeling of nucleation kinetics in experiments for poly-Si growth on SiO_2 by hot wire chemical vapor deposition, *Thin Solid Films*, 458 (1-2): 67-70 JUN 30 2004

10. Christine E. Richardson, Maribeth S. Mason, and Harry A. Atwater. "A Phase Diagram for Morphology and Properties of Low Temperature-Deposited Polycrystalline Silicon Grown by Hot-wire Chemical Vapor Deposition" in *Amorphous and Nanocrystalline Silicon Science and Technology*— 2004, (Mater. Res. Soc. Symp. Proc. 808, Warrendale, PA, 2004).

11. Christine Esber Richardson, B.M. Kayes, M.J. Dicken, and Harry A. Atwater. "A Phase Diagram of Low Temperature Epitaxial Silicon Grown by Hot-wire Chemical Vapor Deposition for Photovoltaic Devices" in *Amorphous and Nanocrystalline Silicon Science and Technology*-2005, (Mater. Res. Soc. Symp. Proc. 862, Warrendale, PA, 2005).

12. Christine Esber Richardson, M.S. Mason and Harry A. Atwater. "A Phase Diagram for Morphology and Properties of Low Temperature Deposited Polycrystalline Silicon Grown by Hot-wire Chemical Vapor Deposition." *Proceedings of the 31st IEEE Photovoltaics Specialists Conference.* Lake Buena Vista, FL. (2005)

13. Mason, MS; Richardson, CE; Atwater, HA; Ahrenkiel, RK, Microsecond minority carrier lifetimes in HWCVD-grown films and implications for thin film solar cells, *Thin Solid Films*, 501 (1-2): 288-290 APR 20 2006

14. Richardson, CE; Mason, MS; Atwater, HA, Hot-wire CVD-grown epitaxial Si films on Si(100) substrates and a model of epitaxial breakdown, *Thin Solid Films*, 501 (1-2): 332-334 APR 20 2006

15. Richardson, CE; Park, YB; Atwater, HA; Surface evolution during crystalline silicon film growth by low-temperature hot-wire chemical vapor deposition on silicon substrates, *Physical Review B*, 73 (24): Art. No. 245328 JUN 2006

16. C. E. Richardson, Y.-B. Park, and H. A. Atwater, "Surface Evolution during LowTemperature Epitaxial Silicon Growth by Hot-wire Chemical Vapor Deposition: Structural and Electronic Properties." *Proceedings of the 4th IEEE Photovoltaics Specialists Conference.*Waikoloa, HI. (2006)

Presentations under Subcontract

1. "Hot-Wire Chemical Vapor Deposition of High Hydrogen Content Silicon Nitride for Crystalline Silicon Solar Cells", J. K. Holt, D. G. Goodwin, A. M. Gabor, M. Stavola, and Harry A. Atwater, 12th Workshop on Crystalline Silicon Solar Cell Materials and Processes, Breckenridge, CO, August 12th, 2002.

2. "Hot-Wire Chemical Vapor Deposition of High Hydrogen Content Silicon Nitride for Solar Cell Passivation and Anti-Reflection Coating Applications", J. K. Holt, D. G. Goodwin, A. M. Gabor, M. Stavola, and Harry A. Atwater, 2nd International Conference on CAT-CVD (Hot Wire Chemical Vapor Deposition), Denver, CO, September 10th, 2002.

3. "Hot-Wire Chemical Vapor Deposition of Silicon and Silicon Nitride", Harry Atwater, <u>invited</u> talk at PolySE, International Conference on Polycrystalline Semiconductors, Nara City, Japan, September 10th, 2002.

4. "Hot-Wire Chemical Vapor Deposition of Silicon and Silicon Nitride", Harry Atwater, <u>invited talk</u>, MRS Symposium A: Amorphous and Nanocrystalline Silicon-Based Films 2003, Spring 2003 Materials Research Society Meeting, San Francisco, CA, April 21st – 25th, 2003.

5. "Hot-Wire Chemical Vapor Deposition for Epitaxial Silicon Growth on Large-Grained Polycrystalline Silicon Templates" M.S. Mason, C.M. Chen, and H.A. Atwater, MRS Symposium A: Amorphous and Nanocrystalline Silicon-Based Films 2003, Spring 2003 Materials Research Society Meeting, San Francisco, CA, April 21st – 25th, 2003.

6. "Microstructure and Passivation in Silicon-Based Thin Film Polycrystalline and Nanostructured Solar Cells. Harry Atwater, <u>invited talk</u>, Symposium V "Critical Interfacial Issues in Thin-Film Optoelectronic and Energy Conversion Devices", Fall 2003 Materials Research Society Meeting, Boston MA, December 1st – 5th, 2003.

7. "A Phase Diagram for Morphology and Properties of Low Temperature-Deposited Polycrystalline Silicon Grown by Hot Wire Chemical Vapor Deposition", Christine Esber Richardson, Maribeth Swiatek Mason and Harry A Atwater, Symposium A, Amorphous and Nanocrystalline Silicon Science and Technology-2004, Spring 2004 Materials Research Society Meeting, San Francisco, CA, April 12 - 16, 2004.

8. C. E. Richardson, Y.-B. Park, and H. A. Atwater, "Surface Evolution during Low Temperature Epitaxial Silicon Growth by Hot-wire Chemical Vapor Deposition: Structural and Electronic Properties." Proceedings of the 4th IEEE Photovoltaics Specialists Conference. Waikoloa, HI. (2006)

9. Christine E. Richardson, M.S. Mason and Harry A. Atwater. "Hot-wire CVD Grown Epitaxial Films and a Model of Epitaxial Breakdown." 3rd International Conference on CAT-CVD (Hot Wire Chemical Vapor Deposition), Utrecht Netherlands, August 23 – 27, 2004.

10. Maribeth S. Mason, C. E. Richardson, Harry A. Atwater, R.K. Ahrenkiel. "Microsecond Minority Carrier Lifetimes in HWCVD-Grown Films and Implications for Thin Film Solar Cells." 3rd International Conference on CAT-CVD (Hot Wire Chemical Vapor Deposition), Utrecht Netherlands, August 23 – 27, 2004.

11. Christine E. Richardson, J. K. Holt, and Harry A. Atwater. "Epitaxial Silicon and Silicon Nitride Growth by Hot-wire Chemical Vapor Deposition for Photovoltaic Devices." 15th Workshop on Crystalline Si Solar Cells. Vail, CO. August 8th - 12th, 2005

12. "Large-Grained Polycrystalline Films for Photovoltaic Devices", Christine Esber Richardson and Harry A. Atwater, Amorphous and Nanocrystalline Silicon Science and Technology-2005, Spring 2005 Materials Research Society Meeting, San Francisco, CA, March 28th – April 1st, 2005.

13. "Morphology and Properties of Low Temperature Deposited Polycrystalline Silicon Grown by Hot-wire Chemical Vapor Deposition." 31st IEEE Photovoltaics Specialists Conference. Lake Buena Vista, FL. January 3-7, 2005.

14. Christine E. Richardson, Maribeth S. Mason, and Harry A. Atwater. "A Phase Diagram of Hot-wire CVD Epitaxial Si Films on Si (100) Substrates and Large-grained Polycrystalline Templates." *14th Workshop on Crystalline Si Solar Cells.* Winterpark, CO. August 8 – 11, 2004

15. Christine E. Richardson, Maribeth S. Mason, and Harry A. Atwater. "A Phase Diagram for Morphology and Properties of Low Temperature-Deposited Polycrystalline Silicon Grown by Hot-wire Chemical Vapor Deposition" in *Amorphous and Nanocrystalline Silicon Science and Technology*— 2004, Spring 2004 Materials Research Society Meeting, San Francisco, CA, April 12th – 16th, 2004.

16. "Silicon Thin Film Photovoltaic Devices" Harry Atwater, NSF Workshop on Nanotechnology for Energy Sciences, November 21st, 2005, Arlington, VA,

17. "Surface Evolution During Epitaxial and Polycrystalline Silicon Film Growth by Low Temperature Hot-Wire Chemical Vapor Deposition on Silicon Substrates" Christine Esber Richardson, Young-bae Park and Harry A Atwater, Symposium A: Amorphous and Polycrystalline Thin-Film Silicon Science and Technology,

Spring 2006 Materials Research Society Meeting, San Francisco, CA, April 17th –
21st, 2006.

Honors and Awards under Subcontract

1. Harry Atwater, Howard Hughes Chaired Professorship, California Institute of
Technology, 2002.
2. Christine M. Richardson, Best Young Researcher Award, 3rd International
Conference on CAT-CVD (Hot Wire Chemical Vapor Deposition), Utrecht
Netherlands, August 23 – 27, 2004.
3. Harry Atwater Joop Los Award and Fellowship, Dutch Foundation for
Fundamental Research on Matter, 2004.
4. Christine M. Richardson, National Physical Sciences Consortium Fellowship,
2003.
5. Christine M. Richardson, Graduate Student Award, Spring 2005 Materials
Research Society Meeting, San Francisco, CA, March 28th – April 1st, 2005.

REPORT DOCUMENTATION PAGE

Form Approved
OMB No. 0704-0188

The public reporting burden for this collection of information is estimated to average 1 hour per response, including the time for reviewing instructions, searching existing data sources, gathering and maintaining the data needed, and completing and reviewing the collection of information. Send comments regarding this burden estimate or any other aspect of this collection of information, including suggestions for reducing the burden, to Department of Defense, Executive Services and Communications Directorate (0704-0188). Respondents should be aware that notwithstanding any other provision of law, no person shall be subject to any penalty for failing to comply with a collection of information if it does not display a currently valid OMB control number.
PLEASE DO NOT RETURN YOUR FORM TO THE ABOVE ORGANIZATION.

1. REPORT DATE *(DD-MM-YYYY)*	2. REPORT TYPE	3. DATES COVERED *(From - To)*
November 2007	Subcontract Report	March 18, 2007

4. TITLE AND SUBTITLE	5a. CONTRACT NUMBER
Si Passivation and Chemical Vapor Deposition of Silicon Nitride: Final Technical Report, March 18, 2007	DE-AC36-99-GO10337

5b. GRANT NUMBER

5c. PROGRAM ELEMENT NUMBER

6. AUTHOR(S)	5d. PROJECT NUMBER
H.A. Atwater	NREL/SR-520-42325

5e. TASK NUMBER
PVA72101

5f. WORK UNIT NUMBER

7. PERFORMING ORGANIZATION NAME(S) AND ADDRESS(ES)	8. PERFORMING ORGANIZATION REPORT NUMBER
Thomas J. Watson Laboratory of Applied Physics California Institute of Technology Pasadena, California 91125	AAT-2-31605-01

9. SPONSORING/MONITORING AGENCY NAME(S) AND ADDRESS(ES)	10. SPONSOR/MONITOR'S ACRONYM(S)
National Renewable Energy Laboratory 1617 Cole Blvd. Golden, CO 80401-3393	NREL

11. SPONSORING/MONITORING AGENCY REPORT NUMBER
NREL/SR-520-42325

12. DISTRIBUTION AVAILABILITY STATEMENT
National Technical Information Service
U.S. Department of Commerce
5285 Port Royal Road
Springfield, VA 22161

13. SUPPLEMENTARY NOTES
NREL Technical Monitor: Richard Matson/Fannie Posey-Eddy

14. ABSTRACT *(Maximum 200 Words)*
This report investigated chemical and physical methods for Si surface passivation for application in crystalline Si and thin Si film photovoltaic devices. Overall, our efforts during the project were focused in three areas: i) synthesis of silicon nitride thin films with high hydrogen content by hot-wire chemical vapor deposition; ii) investigation of the role of hydrogen passivation of defects in crystalline Si and Si solar cells by out diffusion from hydrogenated silicon nitride films; iii) investigation of the growth kinetics and passivation of hydrogenated polycrystalline. Silicon nitride films were grown by hot-wire chemical vapor deposition and film properties have been characterized as a function of SiH_4/NH_3 flow ratio. It was demonstrated that hot-wire chemical vapor deposition leads to growth of SiN_x films with controllable stoichiometry and hydrogen.

15. SUBJECT TERMS
PV; silicon; hot-wire chemical vapor deposition; nitride; solar cells; stoichiometry; defects; surface passivation; crystalline Si; thin Si film; hydrogen passivation; growth kinetics;

16. SECURITY CLASSIFICATION OF:			17. LIMITATION OF ABSTRACT	18. NUMBER OF PAGES	19a. NAME OF RESPONSIBLE PERSON
a. REPORT	b. ABSTRACT	c. THIS PAGE	UL		
Unclassified	Unclassified	Unclassified			19b. TELEPHONE NUMBER *(Include area code)*

Standard Form 298 (Rev. 8/98)
Prescribed by ANSI Std. Z39.18

F1146-E(09/2007)